Microchim Acta (2015) 182:789–796
DOI 10.1007/s00604-014-1389-0

ORIGINAL PAPER

# Chemiluminescence reaction of glucose-derived graphene quantum dots with hypochlorite, and its application to the determination of free chlorine

**Tooba Hallaj · Mohammad Amjadi · Jamshid L. Manzoori · Roghayeh Shokri**

Received: 18 June 2014 / Accepted: 8 October 2014 / Published online: 1 November 2014


**Abstract** Graphene quantum dots (GQDs) were prepared by a new and facile procedure, and their chemiluminescence (CL) reaction with hypochlorite was studied. It was found that hypochlorite can directly oxidize GQDs to give rise to CL emission, and that the surfactant cetyl trimethyl ammonium bromide enhances CL by a factor of about 18. CL and fluorescence spectra were acquired, and the effect of radical scavengers on the reaction was studied. This CL system was used to develop a simple and sensitive method for the determination of hypochlorite in the 0.5 μM to 1.0 mM concentration range, with a detection limit of 0.3 μM. The method was successfully applied to the determination of free chlorine in (spiked) samples of tap water and pool water.

**Keywords** Graphene quantum dots · Chemiluminescence · Hypochlorite · Nanomaterial

## Introduction

Graphene quantum dots (GQDs), as a recently discovered member of luminescent carbon nanomaterials, have attracted considerable interest in various areas of analytical chemistry. They are graphene fragments with a size distribution below 100 nm, which exhibit pronounced exciton confinement and quantum size effects. As a result, GQDs have non-zero band gap and show intense and stable photoluminescence. Furthermore, GQDs have some other interesting properties such as low toxicity, excellent solubility in various solvents, chemical inertia, and high electrical and thermal conductivity. It should be mentioned that unlike carbon dots which mainly contain amorphous carbon, GQDs have clear graphene lattices inside the dots. Moreover, compared to carbon dots, GQDs have higher surface areas, larger diameters and better surface grafting properties [1, 2].

Chlorine has been extensively used as disinfectants in treating drinking and swimming pool water. Chlorine is usually applied to water in its molecular or hypochlorite form. It initially undergoes hydrolysis to form free chlorine consisting of aqueous molecular chlorine, hypochlorous acid, and hypochlorite ion. High excess of active chlorine in water is harmful to human health and must be avoided [3, 4]. Therefore the monitoring of free chlorine concentration in water samples has appeared of great importance and various analytical methods including chromatography [5, 6], electrochemistry [7, 8], spectrophotometry [9, 10], fluorescence [11, 12] and chemiluminescence (CL) [13–17] have been reported for this purpose.

In recent years, due to the unique physicochemical properties of nanomaterials, many CL systems based on different kinds of nanomaterials have been developed [18, 19]. More recently, the application of luminescent carbon nanomaterials in CL [20–32] and electrochemiluminescence [33] reactions has been investigated. Carbon nanomaterials could participate in a CL reaction as emitting species, after direct oxidation [20–26]; as catalysts of reactions involving other luminophores [27–29]; or as emitters after CL energy transfer [24, 25, 30–32]. Hypochlorite has been used as an oxidant in various chemiluminescent reactions [34] but its effect on the luminescent carbon nanomaterials has not yet been studied.

In this work, we synthesized the GQDs by simple pyrolysis of glucose as a carbon source. It was found that $ClO^-$ as an oxidant is able to directly elicit a CL from the prepared GQDs.

**Electronic supplementary material** The online version of this article (doi:10.1007/s00604-014-1389-0) contains supplementary material, which is available to authorized users.

T. Hallaj · M. Amjadi (✉) · J. L. Manzoori · R. Shokri
Department of Analytical Chemistry, Faculty of Chemistry, University of Tabriz, Tabriz 5166616471, Iran
e-mail: amjadi@tabrizu.ac.ir

The CL intensity of the GQD/ $ClO^-$ reaction is greatly enhanced by addition of cetyl trimethyl ammonium bromide (CTAB). On the basis of this CL system, a simple and sensitive method was established for the determination of $ClO^-$ in tap and pool water samples.

## Experimental

### Apparatus

The CL signals were monitored by LUMAT LB 9507 chemiluminometer (Berthold; www.berthold.com). The luminometer was equipped with an automatic injector functioning on the basis of JET injection technology® and being used for injecting the oxidant. The fluorescence spectra were recorded by RF-540 spectrofluorimeter (Shimadzu, Japan; www.shimadzu.com). CL spectrum was also recorded by this instrument using flow mode with the excitation light source being turned off. UV–vis spectra were recorded on a Cary-100 Spectrophotometer (Varian; www.varianinc.com). The size and shape of GQDs were characterized by transmission electron microscopy (TEM, Leo 906, Zeiss, Germany). The Fourier transform infrared (FTIR) spectrum was recorded on a FT-IR spectrophotometer (Tensor 27, Bruker; www.bruker.com). X-ray powder diffraction (XRD) pattern was measured by a Siemens D 500 instrument (Germany). Raman spectrum was recorded using an Almega Thermo Nicolet Dispersive Raman Spectrometer with a 532 nm laser.

### Reagents

All reagents were of analytical-reagent grade. Doubly distilled deionized water (obtained from Ghazi Serum Co. Tabriz, Iran) was used throughout the experiment. Glucose, di-sodium phosphate and CTAB were purchased from Merck (Darmstadt, Germany, www.merck-chemicals.com). A stock standard solution of 0.1 M of NaClO was daily prepared by diluting the appropriate amount of 5 % NaClO solution (standardized by iodometric titration) in 25 mL of deionized water. Working solutions were prepared by appropriate dilution of the stock solution.

### Synthesis of GQDs

GQDs were synthesized by pyrolyzing glucose. In a typical procedure, 6.0 g of glucose was put into a glass beaker and heated on a hot plate at 180 °C until the glucose powder was melted. After about 1.5 min, the color of liquid was changed from colorless to orange. This color change implies the formation of GQDs. At this stage, the heating was stopped and 25 mL of deionized water was added into the orange liquid with continuous and vigorous stirring. The obtained GQD solution was stable for more than 1 month in the refrigerator at 4 °C.

### General procedure for CL monitoring

CL measurements were conducted on the batch condition with the automatic injection system, which provides high speed and repeatable and efficient mixing of the reagents. An amount of 400 μL of GQDs, 100 μL of phosphate buffer (0.1 M, pH=8) and 100 μL of CTAB solution (0.25 M) were added into the cell (a tube with 75 mm height and 12 mm diameter) and the final volume was reached to 700 μL with deionized water. After injection of 300 μL of standard or sample $ClO^-$ solution by the automatic injector, the CL signal was automatically monitored versus time. Maximum CL intensity was used as the analytical signal.

### Procedure for water samples

No pretreatment was necessary for tap water. Pool water was diluted 5-fold. 300 μL of water samples was taken for analysis according to the general procedure.

## Results and discussion

### Synthesis and characterization of GQDs

In this work, a simple carbonization method was used for synthesis of GQDs using glucose as a carbon source. Glucose has previously been used for preparation of GQDs by microwave-assisted hydrothermal method [35]. However, we found that its direct pyrolysis is a much simpler procedure for obtaining GQDs. Various amounts of glucose was tested for pyrolysis and found that when 6 g of glucose was pyrolyzed and its volume was reached to 25 mL, the highest fluorescence was obtained. Also the influence of time and temperature of heating was studied and found that 1.5 min heating at 180 °C is the best conditions. At longer and shorter times, the fluorescence of obtained GQDs is decreased. The TEM image of GQDs synthesized by the suggested procedure shows that they are of spherical shape and nearly monodisperse with size distribution of 20±5 nm (Fig. 1a). As shown in Fig. 1b, the XRD pattern of GQDs exhibits a broad (002) peak around 20° (0.44 nm), corresponding to the graphite structure. This is in a good agreement with the reported values for GQDs prepared by hydrothermal method [35]. FTIR spectroscopy was applied to characterize the functional groups of the prepared GQDs (Fig. 1c). The peaks at 1,643 and 1,710 $cm^{-1}$ are attributed to C = C and C = O stretching vibrations, respectively and the peaks at about 1,364 and 2,894 $cm^{-1}$ to the stretching vibration of C–H. The broad intense peak at

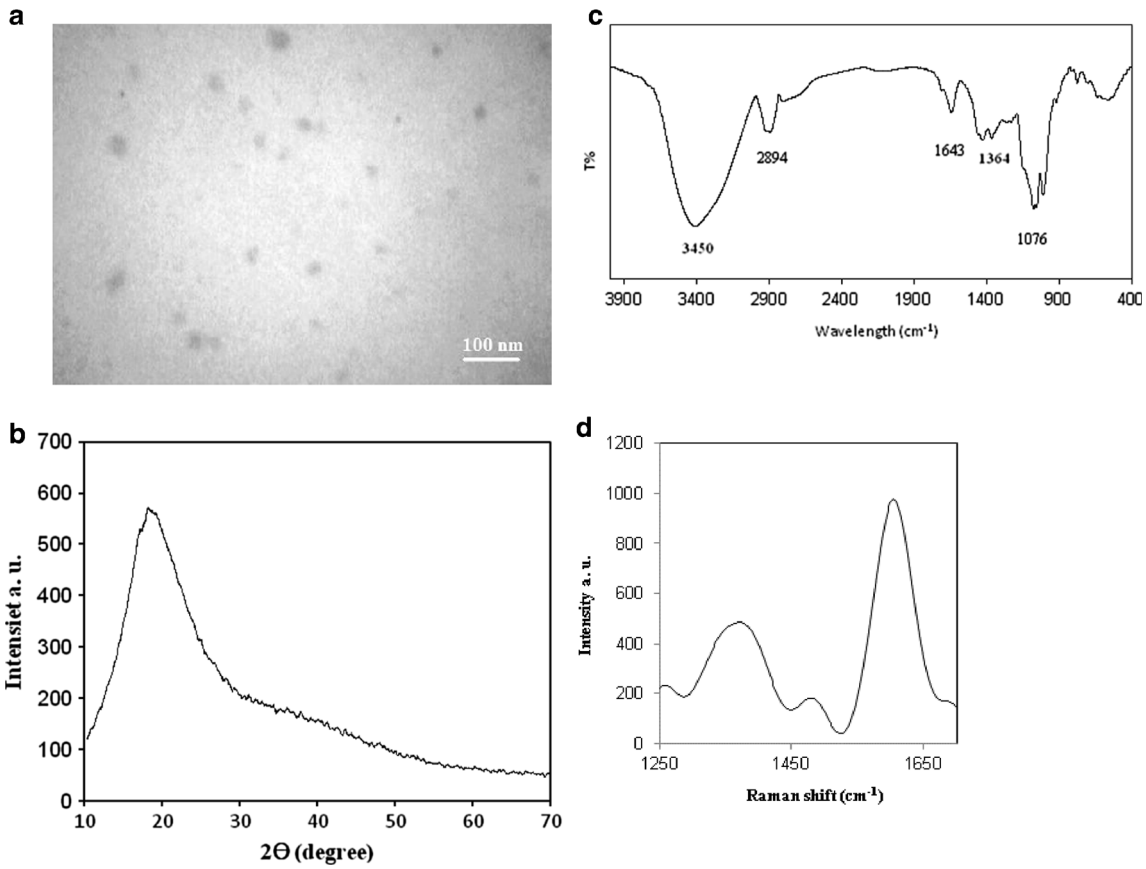


**Fig. 1** **a** TEM image, **b** XRD pattern, **c** FT-IR spectrum and **d** Raman spectrum of the prepared GQDs

3,450 $cm^{-1}$ is assigned to O-H stretching vibrations. Additionally, the peak at 1,076 $cm^{-1}$ reveals the existence of C-O bonding.

Raman spectrum of the synthesized GQDs (Fig. 1d) exhibits two characteristic peaks around 1,370 and 1,605 $cm^{-1}$, corresponding to the D and G band of graphene, respectively. The D band arising from a breathing mode of k-point phonons of $A_{1g}$ symmetry and a G corresponds to the first-order scattering of the $E_{2g}$ vibration mode. The prepared GQDs exhibit small $I_D/I_G$ value of about 0.5, which indicates the high quality of crystalline graphitic system [1].

The UV–vis absorption spectrum of GQDs (Fig. 2a) exhibits typical absorption of graphene derivatives in the UV region with a peak at ~226 nm which was assigned to the π–π* transition of C = C and a peak at ~282 nm corresponds to the n–π* transition of C = O. The fluorescence emission of the GQDs was also investigated. The maximum fluorescence wavelength was ~475 nm, which obtained with an excitation wavelength of 400 nm. As shown in Fig. 2b the GQDs exhibit an excitation-dependent photoluminescence behavior i.e. when the excitation wavelength changes from 350 to 450 nm, the emission peak shifts to longer wavelengths. The obtained results were similar to those previously reported in literature and confirm the proper synthesis of GQDs [35].

## Kinetic profile of CL

Our preliminary experiments indicated that $ClO^-$ is able to directly elicit a CL from GQDs, though the CL intensity was weak (Fig. 3a). However, in CTAB micellar medium CL is greatly enhanced (about 18-fold) (Fig. 3b). The control experiments showed that the coexisting substrates have low or no CL emission upon reaction with $ClO^-$. The kinetic profile of GQDs/$ClO^-$ CL system (Fig. 3) showed that the CL reaction was very fast and the intensity reached a maximum value within 1 s after injection of the oxidant.

## Possible mechanism of CL reaction

In order to explain the CL reaction mechanism and identify the emitting species, following experiments were performed. Firstly, the CL spectrum of GQDs/$ClO^-$/CTAB system was recorded using a spectrofluorimeter in flow mode. The obtained spectrum (Fig. 4a) indicated that there was an emission band in the range of 400–600 nm with a maximum at ~510 nm. This CL spectrum is similar to the GQD fluorescence spectrum (Fig. 4b). Therefore, the CL can be attributed to the excited GQDs.

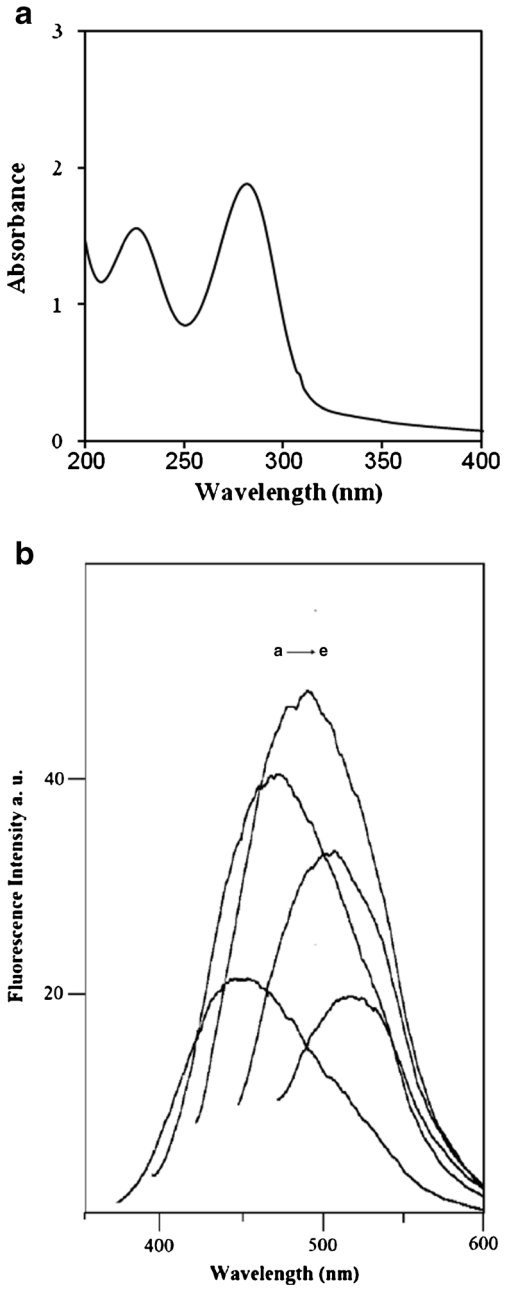


**Fig. 2** **a** UV–vis absorption spectrum of GQDs. **b** Fluorescence spectra for GQDs excited at 350–450 nm wavelength range, with increments of 25 nm

Moreover, the fluorescence spectrum of GQDs after mixing with $ClO^-$ was recorded. According to the results, after addition of $ClO^-$ to GQD solution, the fluorescence intensity at 510 nm decreased. So it can be concluded that a chemical reaction occurred between GQDs and $ClO^-$. Finally the effect of some radical scavengers including NaN3, thiourea, quercetin and ascorbic acid on the CL intensity of GQD/$ClO^-$/CTAB system was investigated. The results of this study together with possible reaction pathways are described in Electronic Supplementary Material (ESM).

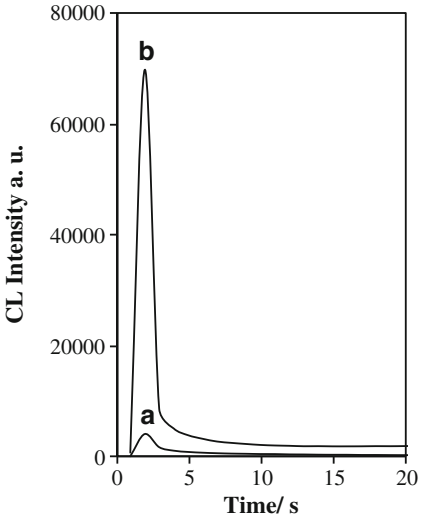


**Fig. 3** Kinetic curve for GQDs/$ClO^-$ CL system (**a**) alone, (**b**) in the presence of CTAB. Conditions: GQDs, 400 μL, phosphate buffer (0.01 M, pH=8), CTAB (0.025 M) and $ClO^-$ ($10^{-3}$ M)

## Effects of variables on the CL intensity

According to the above-mentioned findings, a new CL system could be developed for the determination of $ClO^-$. To establish the optimal conditions for the analysis of $ClO^-$, the effects of several analytical variables such as the pH value, buffer and surfactant concentration and the amount of GQD solution on the CL intensity were investigated.

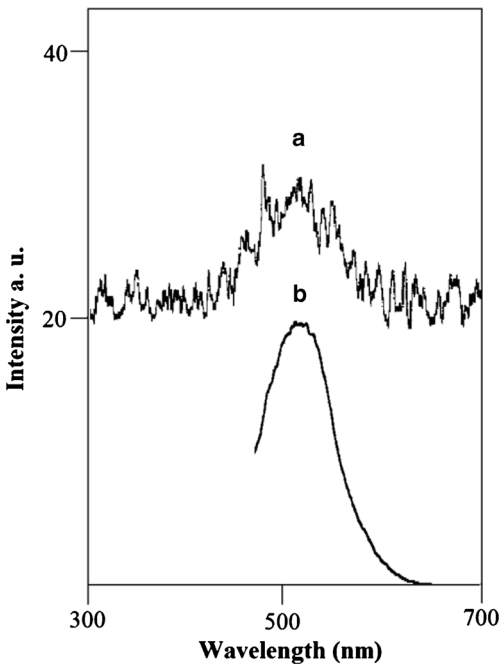


**Fig. 4** **a** CL spectrum of GQDs/$ClO^-$/CTAB system, obtained with continuous flow of reagents: GQD solution, phosphate buffer (0.02 M, pH=8) and CTAB (0.05 M) in one line and $ClO^-$ ($2\times10^{-3}$ M) in other line; **b** fluorescence spectrum of GQDs, at $\lambda_{ex}$=450 nm

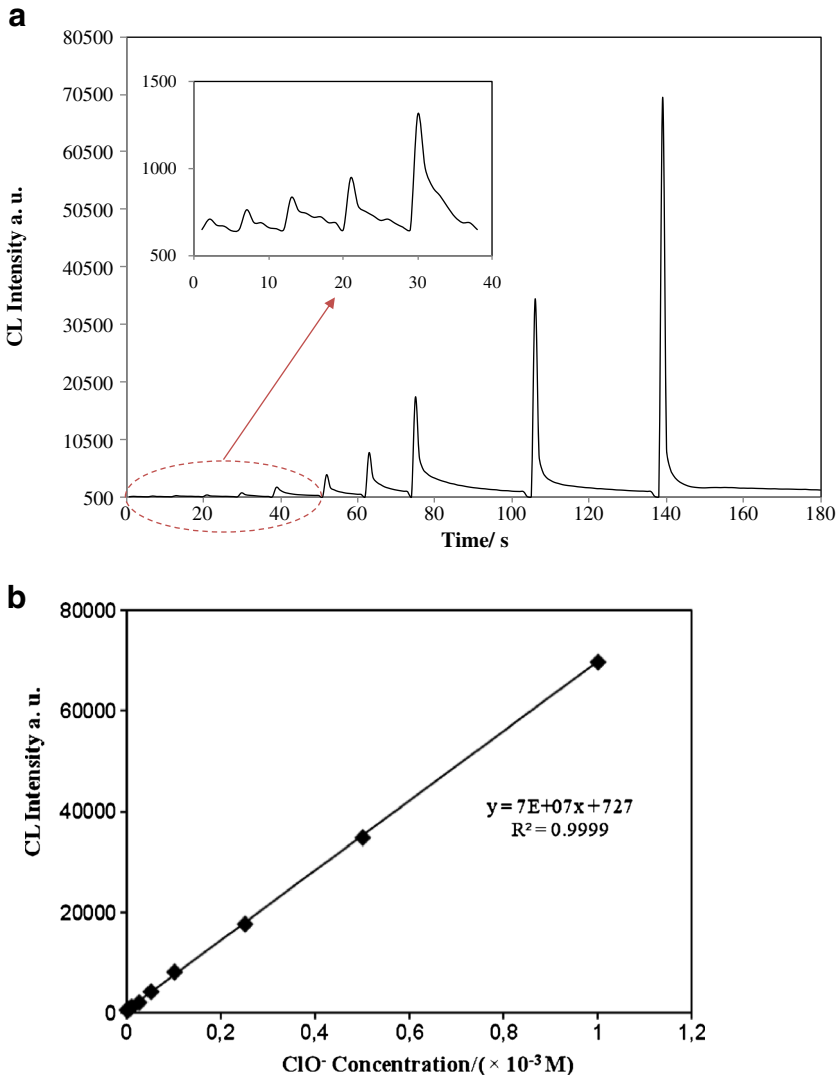


**Fig. 5** **a** CL signals and **b** calibration curve for $ClO^-$ in the range from $5\times10^{-7}$ to $10^{-3}$ M. Conditions: GQD (400 μL), phosphate buffer (0.01 M, pH= 8), CTAB (0.025 M)

The CL intensity is highly sensitive to the pH value. In order to obtain the suitable medium for CL reaction, the pH of GQD/$ClO^-$ /CTAB reaction mixture was varied in the range of 4–11. The results in Fig. S1a (ESM) indicated that the CL intensity increased with pH and reached a maximum around pH 8. This may be attributed to the fact that the production of peroxyacids from the surface carboxylate groups of the GQDs would be most efficient at this pH where the parent carboxylic acid is fully dissociated while the chlorine is still in the form of hypochlorous acid [13].

Moreover, the effect of phosphate buffer concentration on the CL signal was studied and the results are shown in Fig. S1b (ESM). As seen, the CL intensity increased by increasing phosphate buffer concentration up to 0.01 M, and then remained constant.

**Table 1** Comparison of the developed CL method for the determination $ClO^-$ with some previously published CL methods

| CL system | LOD (M) | Linear range (M) | Ref |
|---|---|---|---|
| Poly(Luminol)-$ClO^-$-$H_2O_2$ | $5\times10^{-7}$ | $5\times10^{-7}$–$4\times10^{-3}$ | [17] |
| Luminol-$ClO^-$ | – | $1\times10^{-7}$–$1\times10^{-4}$ | [14] |
| bis(2,4,6(trichlorophenyl)oxalate)-$ClO^-$ | $2\times10^{-6}$ | $2\times10^{-6}$–$3\times10^{-5}$ | [16] |
| Fluoresceinate- $ClO^-$ | $5.3\times10^{-6}$ | $1.5\times10^{-4}$–$6.9\times10^{-4}$ | [15] |
| Uranine- $ClO^-$ | $3\times10^{-6}$ | $2\times10^{-6}$–$1\times10^{-3}$ | [37] |
| Rhodamine 6G- $ClO^-$ | $1.2\times10^{-6}$ | – | [13] |
| GQD- $ClO^-$ | $3\times10^{-7}$ | $5.0\times10^{-7}$–$1\times10^{-3}$ | This work |

**Table 2** Tolerance limit of interferences on the determination of $1\times10^{-5}$ M $ClO^-$

| Interfering species | Tolerance (M) |
|---|---|
| $Na^+$, $K^+$, $Ba^{2+}$, $SO_4^{2-}$, $NO_3^-$, $CO_3^{2-}$, $F^-$, $Br^-$,$Cl^-$ | $1\times10^{-3}$ |
| $Mg^{2+}$, $Ca^{2+}$, $Al^{3+}$, $Ag^+$, $Fe^{3+}$ | $5\times10^{-4}$ |
| $Zn^{2+}$, $Co^{2+}$, $Cr^{3+}$, $Pb^{2+}$ | $1\times10^{-4}$ |
| $Cu^{2+}$, $I^-$ | $5\times10^{-5}$ |
| Humic acid | 5 mg $L^{-1}$ |

Surfactants at concentrations above its critical micellar concentration (CMC) usually enhance the CL emission in many reactions [36]. Therefore, the effects of three kinds of surfactants including cationic (CTAB), anionic (sodium dodecyl sulfate, SDS), and nonionic surfactants (Triton X-100), on the GQD/$ClO^-$ CL system were investigated. The CL signal was remarkably enhanced in the presence of CTAB. However, SDS and Triton X-100 did not show significant influence on the GQD/ $ClO^-$ system. Therefore, CTAB was chosen as a suitable surfactant for the CL enhancement. The maximum CL intensity was obtained at $2.5\times10^{-2}$ M CTAB concentration (Fig. S1c, ESM). Two phenomena may be involved in the enhancement effect of CTAB micelles on the CL system. First, the micelle surfaces which are rich in positive charge can attract and concentrate the superoxide anion radicals to providing more reaction opportunities. Second, the micelles protect the excited state GQDs and decrease the non-radiative transitions which lead to a significant increase in the CL intensity.

Finally, the effect of the amount of GQD solution on the CL intensity was investigated in the range of 50–700 μL of stock solution. As shown in Fig. S1d (ESM), the CL intensity increased by increasing GQD volume up to 400 μL and then remained relatively constant. Therefore, this amount was selected as the optimum value for experiments.

## Analytical figures of merit

Under the optimized experimental conditions, the CL intensity was proportionally increased with concentration of free chlorine (Fig. 5a). The linear range was $5\times10^{-7}$ to $1\times10^{-3}$ M with a detection limit of (3 s) of $3\times10^{-7}$ M (Fig. 5b). The regression equation was $I=(7\times10^7)$ C + 727, $R^2=0.9999$, where I is CL intensity and C is concentration of $ClO^-$ (M). The relative standard deviation (RSD) was 1.6 % for five determinations of $1\times10^{-5}$ M $ClO^-$. Table 1 compares the developed method with some other reported CL methods for the $ClO^-$ determination. As can be seen, the analytical performances of this method are better than or comparable with those of other methods. Moreover, our method is quite simpler and less expensive than most of other methods. Finally, it should be mentioned that GQDs/$ClO^-$ as a novel CL system may have other potential analytical applications.

## Interferences

In order to evaluate the selectivity of the proposed method, the effect of some metal ions and anions commonly present in water samples on the determination of $1.0\times10^{-5}$ M $ClO^-$ was investigated. The tolerable concentrations for interfering species in relative error of <5 % were summarized in Table 2. These results demonstrate that the method possesses a good selectivity for the determination $ClO^-$ in water samples.

## Analysis of water samples

The developed method was applied to the determination of free chlorine in tap and pool water samples. The obtained results are shown in Table 3. In order to confirm the accuracy of method, the results were compared with those obtained by N,N-diethyldiphenylenediamine (DPD) standard method. According to statistical analysis by Student *t*-test, there is no significant difference between the results of two methods (Table 3). In addition, the samples were spiked with known amounts of $ClO^-$, and then they were analyzed according to the general procedure. The obtained results (Table 3) indicated that there are no significant differences between the added and found values.

**Table 3** Determination of $ClO^-$ in tap and pool water samples

| Sample | Added (μM) | Found (μM)[a] | Recovery (%) | Found (Official method) (μM) | t-statistic[b] |
|---|---|---|---|---|---|
| Tap water | – | 7.7±0.20 | – | 7.8±0.06 | 1.1 |
| | 5 | 12.8±0.47 | 101.0±3.71 | – | 0.44 |
| | 10 | 17.6±0.33 | 99.8±1.87 | – | 0.21 |
| Pool water | – | 44.7±0.77 | – | 42.8±2.60 | 0.77 |
| | 10 | 54.8±1.54 | 100.1±2.80 | – | 0.1 |
| | 20 | 63.7±1.04 | 98.4±1.63 | – | 1.73 |

[a] Mean of three determinations ± standard deviation

[b] *t*-critical=4.3 for $n=2$, $P=0.05$

## Conclusion

In this work, we demonstrated that GQDs obtained from pyrolysis of glucose could be directly oxidized by $ClO^-$ to give rise to the CL emission. The CL was supposed to be originated from the processes of electron transfer annihilation and resonance energy transfer. Additionally, it was found that CTAB could remarkably enhance the CL intensity of GQD/$ClO^-$ system via concentrating of the reactive anion radicals and providing a protective environment for excited state species. The GQD/$ClO^-$ /CTAB CL system was applied to the determination of $ClO^-$ in tap and pool water samples with good accuracy and high precision. Considering the simplicity and reliability of this CL system, it can be used in other analytical applications.

## References


1. Li L, Wu G, Yang G, Peng J, Zhao J, Zhu JJ (2013) Focusing on luminescent graphene quantum dots: current status and future perspectives. Nanoscale 5:4015–4039
2. Shen J, Zhu Y, Yang X, Li C (2012) Graphene quantum dots: emergent nanolights for bioimaging, sensors, catalysis and photovoltaic devices. Chem Commun 48:3686–3699
3. White GC (1972) Handbook of chlorination; for potable water, wastewater, cooling water, industrial processes, and swimming pools. Van Nostrand Reinhold Co, New York
4. World Health Organization (1993) International program on chemical safety, guidelines for drinking-water quality, 2nd edn. World Health Organization, Geneva
5. Wakigawa K, Gohda A, Fukushima S, Mori T, Niidome T, Katayama Y (2013) Rapid and selective determination of free chlorine in aqueous solution using electrophilic addition to styrene by gas chromatography/mass spectrometry. Talanta 103:81–85
6. Jain A, Verma KK (1993) HPLC determination of chlorine in air and water samples following precolumn derivatization to 4-bromoacetanilide. Chromatographia 37:492–496
7. Kishioka S, Kosugi T, Yamada A (2005) Electrochemical determination of a free chlorine residual using cathodic potential-step chronocoulometry. Electroanalysis 17:724–726
8. Nascimento VB, Selva TMG, Coelho ECS, Santos FP, Antônio JLS, Silva JR, Gaião EN, Araújo MCU (2010) Automatic determination of chlorine without standard solutions using a biamperometric flow-batch analysis system. Talanta 81:609–613
9. Melchert WR, Oliveira DR, Rocha FRP (2010) An environmentally friendly flow system for high-sensitivity spectrophotometric determination of free chlorine in natural waters. Microchem J 96:77–81
10. Al-Okab RA, Syed AA (2009) Novel oxidative electrophilic coupling reactions of phenoxazine derivatives with MBTH and their applications to spectrophotometric determination of residual chlorine in drinking water and environmental water samples. J Hazard Mater 170:292–297
11. Dong Y, Li G, Zhou N, Wang R, Chi Y, Chen G (2012) Graphene quantum dot as a green and facile sensor for free chlorine in drinking water. Anal Chem 84:8378–8382
12. Yin B, Deng J, Peng X, Long Q, Zhao J, Lu Q, Chen Q, Li H, Tang H, Zhang Y, Yao S (2013) Green synthesis of carbon dots with down- and up-conversion fluorescent properties for sensitive detection of hypochlorite with a dual-readout assay. Analyst 138:6551–6557
13. Irons GP, Greenway GM (1995) Investigation into the detection of chlorine species by Rhodamine 6G chemiluminescence with electrochemical modification. Analyst 120:477–483
14. Ishimaru N, Lin JM, Yamada M (1998) Luminol-free chlorine chemiluminescence in an oil-in-water microemulsion medium. Anal Commun 35:67–69
15. Ballesta Claver J, Valencia Mirón MC, Capitán-Vallvey LF (2004) Determination of hypochlorite in water using a chemiluminescent test strip. Anal Chim Acta 522:267–273
16. Nakamura MM, Coichev N, Lin JM, Yamada M (2003) Flow-injection investigation of the chemiluminescent reaction of bis(2,4,6-(trichlorophenyl)oxalate) with free chlorine. Anal Chim Acta 484:101–109
17. Szili M, Kasik I, Matejec V, Nagy G, Kovacs B (2014) Poly(luminol) based sensor array for determination of dissolved chlorine in water. Sensors Actuators B 192:92–98
18. Li Q, Zhang L, Li J, Lu C (2011) Nanomaterial-amplified chemiluminescence systems and their applications in bioassays. Trends Anal Chem 30:401–413
19. Giokas DL, Vlessidis AG, Tsogas GZ, Evmiridis NP (2010) Nanoparticle-assisted chemiluminescence and its applications in analytical chemistry. Trends Anal Chem 29:1113–1126
20. Xue W, Lin Z, Chen H, Lu C, Lin JM (2011) Enhancement of ultraweak chemiluminescence from reaction of hydrogen peroxide and bisulfite by water-soluble carbon Nanodots. J Phys Chem C 115:21707–21714
21. Lin Z, Xue W, Chen H, Lin JM (2011) Peroxynitrous-acid-induced chemiluminescence of fluorescent carbon dots for nitrite sensing. Anal Chem 83:8245–8251
22. Lin Z, Xue W, Chen H, Lin JM (2012) Classical oxidant induced chemiluminescence of fluorescent carbon dots. Chem Commun 48:1051–1053
23. Amjadi M, Manzoori JL, Hallaj T, Sorouraddin MH (2014) Direct chemiluminescence of carbon dots induced by potassium ferricyanide and its analytical application. Spectrochim Acta A 122:715–720
24. Amjadi M, Manzoori JL, Hallaj T, Sorouraddin MH (2014) Strong enhancement of the chemiluminescence of the cerium(IV)-thiosulfate reaction by carbon dots, and its application to the sensitive determination of dopamine. Microchim Acta 181:671–677
25. Jiang J, He Y, Li S, Cui H (2012) Amino acids as the source for producing carbon nanodots: microwave assisted one-step synthesis, intrinsic photoluminescence property and intense chemiluminescence enhancement. Chem Commun 48:9634–9636
26. Amjadi M, Manzoori JL, Hallaj T (2014) Chemiluminescence of graphene quantum dots and its application to the determination of uric acid. J Lumin 153:73–78
27. Hao M, Liu N, Ma Z (2013) A new luminol chemiluminescence sensor for glucose based on pH-dependent graphene oxide. Analyst 138:4393–4397
28. Lin Z, Dou X, Li H, Chen Q, Lin JM (2014) Silicon-hybrid carbon dots strongly enhance the chemiluminescence of luminol. Microchim Acta. doi:10.107/f00604-013-1153-x
29. Wang DM, Gao MX, Gao PF, Yang H, Huang CZ (2013) Carbon nanodots-catalyzed chemiluminescence of luminol: a singlet oxygen-induced mechanism. J Phys Chem C 117:19219–19225
30. Dou X, Lin Z, Chen H, Zheng Y, Lu C, Lin JM (2013) Production of superoxide anion radicals as evidence for carbon nanodots acting as electron donors by the chemiluminescence method. Chem Commun 49:5871–5873
31. Shi J, Lu C, Yan D, Ma L (2013) High selectivity sensing of cobalt in HepG2 cells based on necklace model microenvironment-modulated carbon dot-improved chemiluminescence in Fenton-like system. Biosens Bioelectron 45:58–64

32. Zhou Y, Xing G, Chen H, Ogawa N, Lin JM (2012) Carbon nanodots sensitized chemiluminescence on peroxomonosulfate–sulfite–hydrochloric acid system and its analytical applications. Talanta 99:471–477
33. Liang J, Yang S, Luo S, Liu C, Tang Y (2014) Ultrasensitive electrochemiluminescent detection of pentachlorophenol using a multiple amplification strategy based on a hybrid material made from quantum dots, graphene, and carbon nanotubes. Microchim Acta 181:759–765
34. Francis PS, Barnett NW, Lewis SW, Lim KF (2004) Hypohalites and related oxidants as chemiluminescence reagents: a review. Luminescence 19:94–115
35. Tang L, Ji R, Cao X, Lin J, Jiang H, Li X, Teng KS, Luk CM, Zeng S, Hao J, Lau SP (2012) Deep ultraviolet photoluminescence of water-soluble self-passivated graphene quantum dots. ACS Nano 6:5102–5110
36. Lin J (2003) Microheterogeneous systems of micelles and microemulsions as reaction media in chemiluminescent analysis. Trends Anal Chem 22:99–107
37. Nakagama T, Yamada M, Hobo T (1990) Chemiluminescence sensor with uranine immobilized on an anion-exchange resin for monitoring free chlorine in tap water. Anal Chim Acta 231:7–12